Environ Sci Pollut Res (2016) 23:19376–19386
DOI 10.1007/s11356-016-7134-y

RESEARCH ARTICLE

# Depletion of tropospheric ozone associated with mineral dust outbreaks

**Ruben Soler**[1] **· J. F. Nicolás**[1] **· S. Caballero**[1] **· E. Yubero**[1] **· J. Crespo**[1]

Received: 15 April 2016 / Accepted: 20 June 2016 / Published online: 4 July 2016


**Abstract** From May to September 2012, ozone reductions associated with 15 Saharan dust outbreaks which occurred between May to September 2012 have been evaluated. The campaign was performed at a mountain station located near the eastern coast of the Iberian Peninsula. The study has two main goals: firstly, to analyze the decreasing gradient of ozone concentration during the course of the Saharan episodes. These gradients vary from 0.2 to 0.6 ppb $h^{-1}$ with an average value of 0.39 ppb $h^{-1}$. The negative correlation between ozone and coarse particles occurs almost simultaneously. Moreover, although the concentration of coarse particles remained high throughout the episode, the time series shows the saturation of the ozone loss. The highest ozone depletion has been obtained during the last hours of the day, from 18:00 to 23:00 UTC. Outbreaks registered during this campaign have been more intense in this time slot. The second objective is to establish from which coarse particle concentration a significant ozone depletion can be observed and to quantify this reduction. In this regard, it has been confirmed that when the hourly particle concentration recorded during the Saharan dust outbreaks is above the hourly particle median values (N > N-median), the ozone concentration reduction obtained is statistically significant. An average ozone reduction of 5.5 % during Saharan events has been recorded. In certain cases, this percentage can reach values of higher than 15 %.

Responsible editor: Gerhard Lammel

✉ Ruben Soler
ruben87sm@gmail.com

[1] Atmospheric Pollution Laboratory (LCA), Department of Applied Physics, Miguel Hernández University, Avenida de la Universidad S/N, 03202 Elche, Spain

**Keywords** $O_3$ reduction · Mountain station · Saharan dust outbreak · Coarse particles · Mineral dust · Seasonal component

## Introduction

In the Western Mediterranean Basin (WMB), mineral particles and tropospheric ozone are two important components whose atmospheric dynamics are determined by the particular meteorological and orographic conditions that this geographical area presents.

Surface ozone is a secondary pollutant that can cause serious damage to human health, natural vegetation, crops, and materials (Paoletti 2006). Additionally, ozone acts as a potent greenhouse gas due to its ability to absorb light (IPCC 2013). Millán et al. (2000, 2002) and Caballero et al. (2007) describe in detail the complex processes responsible for the accumulation of ozone particularly during spring and summer due to orographic and human factors, and atmospheric dynamics in the WMB. The largest cities of the WMB are mostly located along the coastline, which is surrounded by mountain ranges reaching altitudes of approximately 1500 m. The populations of these cities increase during the summertime and consequently do the emissions of $NO_x$ and other ozone precursors. On summer days, a strong vertical development of an unstable planetary boundary layer aided by the enhancement of coastal and mountain breezes facilitates the transport of these pollutants inland while strong sun insolation promotes their transformation into $O_3$ and other photochemical oxidants (Escudero et al. 2016). When the air masses reach the mountain barrier, whose southern and eastern slopes are strongly heated, these can act as orographic chimneys that favor the return of air masses aloft, with compensatory subsidence over the sea. This process causes the formation of stratified layers that act as reservoirs of aged pollutants, and the ozone in the lowest layers can be transported again by the sea breeze from the coast inland the following morning. As a result of these atmospheric re-circulations, $O_3$ persists along the Mediterranean basin for several days during periods of summer atmospheric stability, and its concentrations frequently exceed the European Community thresholds (Lelieveld et al. 2002; Castell-Balaguer et al. 2012; Escudero et al. 2014).

With regard to the mineral particles, the biggest contribution in the WMB is due to the frequent intrusion of air masses from northern Africa. This transport presents a seasonal trend pointing out a clear maximum during the spring and summer months (Escudero et al. 2005; Querol et al. 2009; Pey et al. 2013). Saharan dust outbreaks (SDOs) that take place during these months show a prevailing meteorological scenario that favors the transport of African dusty air masses towards the WMB. This pattern consists in the development of the North African thermal low caused by the intense heating. The dust is injected into the midtroposphere, and it is transported towards the WMB thanks to a high pressure system (850–700 hPa) (Escudero et al. 2005). Nevertheless, other meteorological patterns throughout the year can take place. These SDOs are primarily responsible for exceedances of the particulate matter (PM) limit value that occur in the regional background stations in this area (Escudero et al. 2007).

Dust particles may also play a significant role as a reactive surface on which heterogeneous chemistry can take place (Adame et al. 2015). Therefore, gaseous pollutants may interact with mineral dust varying their concentrations. Given the importance of these reactions, various studies have been carried out in an attempt to quantify this variation. These assessments have used different approaches. Laboratory experiments and the development of models have been performed (Zhang et al. 1994; Dentener et al. 1996; Zhang and Carmichael 1999; Hanisch and Crowley 2003); results obtained from models have been compared with field-observed data (de Reus et al. 2000; Bauer et al. 2004) and finally, field campaigns have been carried out to register in situ observations (Prospero et al. 1995; Bonasoni et al. 2004; Umann et al. 2005; Andrey et al. 2014; Adame et al. 2015).

These studies show that due to the interaction between mineral dust and ozone, the concentration of ozone decreases. This reduction not only takes place through direct uptake, in which $O_3$ is destroyed on the mineral aerosol surface and $O_2$ is produced (Bauer et al. 2004), but it has also been observed that heterogeneous surface reactions of several gasses on mineral aerosol may also be responsible for the tropospheric $O_3$ decrease. In this way, the depletion of $HNO_3$ and $NO_3$ on dust particles can remove some of the $O_3$ precursors (i.e., $NO_x$) favoring a reduction of photochemical $O_3$ production efficiency (Zhang and Carmichael 1999; Harrison et al. 2001). Under this premise, de Reus et al., 2000 state that both mechanisms, direct removal and heterogeneous removal of nitrogen species, mainly $HNO_3$, accounted for about 50 % of the total net ozone destruction. Umann et al. (2005) obtained an ozone reduction of 33 % during high dust concentration periods, and they confirmed that this decrease stops when the atmospheric $HNO_3$ has been completely removed. The comparison of ozone depletions observed under dust transport episodes, as can be observed during the Saharan dust outbreaks (SDOs), is complex since the timescale in which the ozone reduction is obtained differs among the different studies. In any case, apart from those already mentioned, maximum hourly reductions of 42 % with respect to monthly mean values have been obtained in Mt. Cimone (Italy) (Bonasoni et al. 2004). Depletions in the range of 13.9 to 17.7 % depending on the kind of the monitoring station have been found in southern Italy (Bencardino et al. 2011), comparing days under Saharan dust influence and days without any. On the other hand, Andrey et al. (2014) analyzed numerous ozone vertical profiles and found an ozone peak reduction (35 %) at about 4 km of altitude under Saharan dust outbreak periods in the Canary Islands.

Although it is known that the entry of air masses from the Sahara desert can rise the concentration of both, fine and coarse particles, it is also true that especially in stations located in the Mediterranean basin, the increase recorded by the coarse ones, it is more relevant (Contini et al. 2014; Nicolás et al. 2014; Brattich et al. 2015). Taking into account that the sampling point used in this study is located in the western Mediterranean, we have decided to analyze the interaction ozone-dust mineral only in the coarse fraction (particle size >1 μm) since these particles are the best indicator of SDOs and the main reason for ozone depletion (Bonasoni et al. 2004).

The aim of this work is to quantify the ozone concentrations reductions due to several SDOs detected at a mountain station. The study of interactions between ozone and coarse particles will be based on an hourly time scale allowing for a better observation of its features than with a daily time scale. Time series of ozone concentrations in which its seasonal component was removed have been used and as a result, the effect of the solar radiation on the ozone variability has been minimized. Consequently, ozone reductions shown in the manuscript have very little dependence with the variation of this meteorological variable. This approach has not been addressed in most studies that have dealt with this interaction. Moreover, a particle concentration from which the ozone depletion can be considered statistically significant will be determined.

## Experimental

### Monitoring site and data collection

The sampling site named "Aitana" (38°16'N; 0°41'W; 1558 m a.s.l) is on the top of a mountain range located inland in the province of Alicante, in southeastern Spain. The station is situated 25 km from the Mediterranean coast and about 300 km from the nearest North Africa point (Fig. 1). These features make the station a good receptor of Saharan dust outbreaks. The station is placed inside a military area (EVA n° 5), but the anthropogenic activity in it is scarce. Data concentrations and temporal trends of PM at the site are reported by Nicolás et al. (2014) and Galindo et al. (2016).

The sampling site is mostly (~70 % of days) within the planetary boundary layer (PBL) during the midday in the warm period. Therefore, both particle and ozone concentrations may be affected by recirculation processes. This percentage falls to 30 % in autumn and winter seasons. A detailed characterization of the main meteorological parameters and the PBL dynamics in the study area can be consulted in Galindo et al. (2016).

The instrument used to measure particle concentration was an optical counter Grimm 190, which is able to determine particle number concentrations in 31 particle size channels from 0.25 to 32 μm with a 1-min time resolution. The instrument is based on the quantification of 90° scattering of light by particles. According to the manufacturer, the uncertainty in the particle counting determination is about 5 % and its resolution is 1 particle/liter. Previously to the campaign, the data (in mass

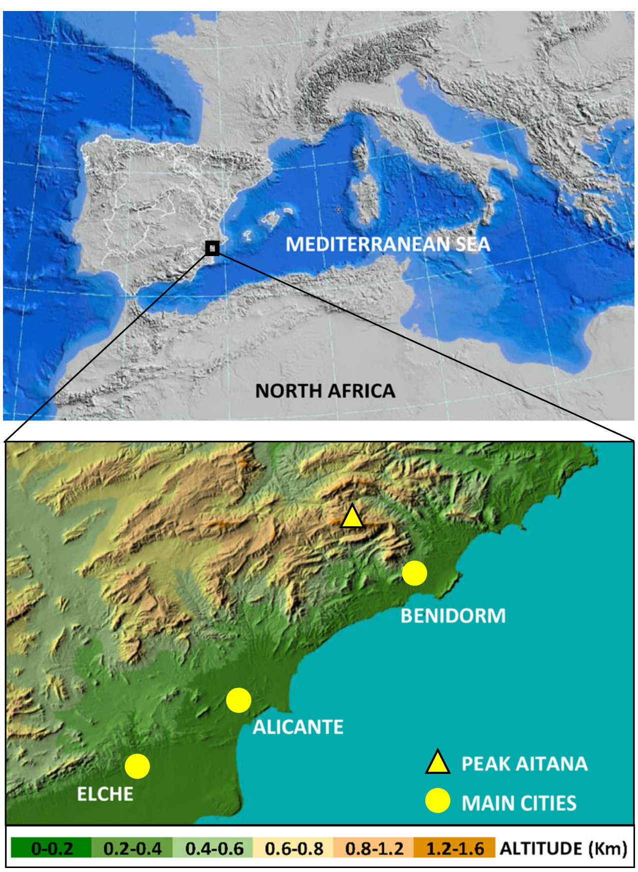


**Fig. 1** Location and topography of the monitoring site on the Spanish Mediterranean coast

concentration) provided by the Grimm spectrometer were verified by comparison with a gravimetric technique to ensure its correct operation. The correlation obtained, $PM_{10}$(Grimm) = 1.11·$PM_{10}$(gravimetric) presented a correlation coefficient of $r = 0.84$.

As aforementioned, only coarse particles (Ncoarse) have been considered in this study. Ncoarse values have been obtained as the result of the particle number concentration addition from each channel from 1 μm. Although it is known that the particles' diameters measured by Grimm change with the refractive index of the aerosol measured (Pio et al. 2014), this is not going to affect the particle number concentration. This effect should be taken into account just in the case the mass concentration is obtained from the number concentration data.

Concentrations of $O_3$ were registered using a Dasibi model 1008 UV absorption continuous analyzer. The analyzer has an accuracy of better than 5 % and 1-min time resolution. Meteorological data (temperature, wind velocity, solar radiation, precipitation, relative humidity) were obtained from a weather station located 10 m above the ground.

The study period comprised from May 2012 to September 2012. It is precisely during these months when the frequency of SDOs in the study area is at its highest during the year.

## Removing the seasonal component of ozone data

The use of daily records to analyze the ozone-particle interaction may hide some of its features. For that reason, hourly data has been used to quantify the depletion of ozone concentrations produced by the interaction with Saharan PM. As such, to remove or at least to reduce the ozone variations due to intrinsic fluctuations, as caused by solar radiation, the hourly seasonal component in ozone data has been obtained using a time series classic model. In this additive model, time series (hourly $O_3$ value) can be considered the sum of three components: a trend component, a seasonal component, and an irregular component. The seasonal component informs us about the part of the ozone's daily oscillatory behavior, mainly due to meteorological variables. Although a well-defined trend component for ozone during the study period was not found, a clear hourly seasonal component was determined.

The seasonal component obtained can be seen in Fig. 2. As it can observe, ozone seasonal component attains a trough (−3.37 ppb) and a peak (+2.08 ppb) at 09:00 and 19:00 h (UTC), respectively. Possibly, this maximum shows the $O_3$ precursors transport from urban coastal areas to the sampling point due to breeze regimen. These hourly concentrations of the seasonal component will be subtracted from the hourly concentration of ozone throughout the whole time series to isolate the daily intrinsic fluctuations.

The hourly concentrations of ozone without this seasonal component will be used to determine a coarse particle concentration from which the ozone depletion can be considered

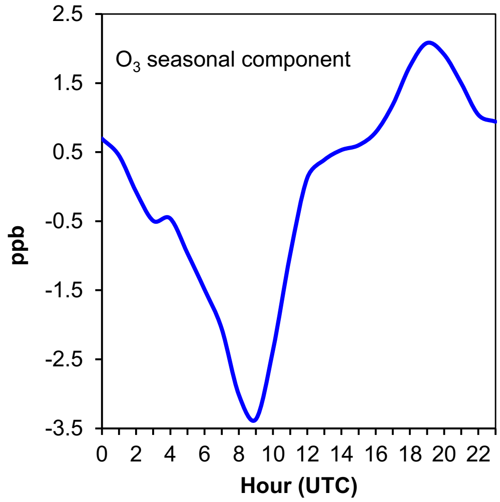


**Fig. 2** Ozone seasonal component obtained from May to September 2012 and applied to hourly ozone data measured at sampling point

statistically significant (section 3.2.2) and to quantify the percentages of this depletion during SDOs (section 3.3).

### SDO identification

The identification of Saharan dust events that passed through the area during the study period was checked in a governmental database (http:www.calima.ws). In that webpage, the identification of SDOs is carried out thanks to dust forecast models (NAAPS, DREAM, and SKIRON) along with a meteorological analysis based on ECMWF model. Moreover, a backtrajectory analysis (HYSPLIT model, Draxler and Rolph 2015) was used to confirm the north-African origin of the air masses during the SDOs identified. Four-day back-trajectories ending in the sampling point at 1500 and 3000 m a.s.l were obtained at 12:00 UTC for these days. The identification is validated by checking the particle concentration time series in regional background stations (RBS). This procedure is based on a methodology for the identification and quantification of the contribution of SDOs developed in Spain and Portugal (Querol et al. 2006). Information about the methodology and the use of the RBS can be consulted in http://ec.europa.eu/environment/air/quality/legislation/pdf/sec_2011_0208.pdf. The SDOs identified according to this method are shown in Table 2.

## Results

### Monthly and hourly ozone and coarse particles variations

Monthly average values of the main meteorological parameters obtained during the study period are shown in Table 1.

**Table 1** Monthly average values for the main meteorological parameters

| | T (°C) | SR (W $m^{-2}$) | v (m $s^{-1}$) | P (mm) | RH (%) |
|---|---|---|---|---|---|
| May-12 | 13.3 | 330.8 | 4.4 | 75.0 | 52.3 |
| Jun-12 | 18.8 | 337.6 | 4.5 | 1.3 | 45.5 |
| Jul-12 | 19.0 | 309.8 | 3.8 | 0.2 | 50.9 |
| Ago-12 | 22.2 | 276.7 | 4.7 | 16.8 | 38.2 |
| Sept-12 | 15.7 | 232.6 | 4.4 | 0.0 | 54.3 |
| Global | 17.8 | 297.8 | 4.4 | 93.3 | 48.0 |

*T* temperature, *SR* solar radiation, *v* wind speed, *RH* relative humidity, *P* total precipitation

The highest temperature value was registered in August, while levels of solar radiation were highest in May and June, with a decrease in September. Although the SR levels always increase from April to May, this year, the SR recorded in May was unusually high. Wind velocity was steady during the whole period. Very little precipitation was registered with most rainfall accumulated during 3 days only (two in May and one in August). Relative humidity showed low monthly average values. Nevertheless, RH can influence measurements in specific hours of day. It is known that optical instruments could be influenced by RH and that the output from these instruments increases with RH (Dinoi et al. 2016). For this reason, hourly particle data recorded with relative humidity higher than 70 % were not taken into account. We have considered this threshold since from values of RH > 70 %, particulate matter absorbs water vapor changing size and optical properties (Dinoi et al. 2016; Donateo et al. 2006). A procedure to correct the effect of RH on concentration measurements can be seen in Donateo et al. 2006.

Figure 3 shows the monthly evolution of the principal statistics parameters for coarse particles and ozone.

In Fig. 3a, it can be observed that the median value of particle concentration in August is between four and five times higher than that obtained in May. Also, the 25th percentile (P25) registered in August presents a similar value to the 75th percentiles (P75) obtained in May and September. These months, May and September, were less influenced by the Saharan dust than the others. A nearly reverse situation is produced in the ozone parameters (Fig. 3b), although the differences between months are not as clear as in the coarse particles case. The high ozone concentration obtained in May (57.5 ppb-median value) is associated with enhanced photochemical activity. An increase in solar radiation compared to April photodissociate to a greater extent the $NO_2$ that is accumulated during winter time (Monks 2000; Ribas and Peñuelas 2004; Escudero et al. 2016). Ozone concentration obtained in August (54.1 ppb-median value) is lower than in September (58.9 ppb-median value) and, therefore, is lower than expected considering the typical ozone trend in summer.

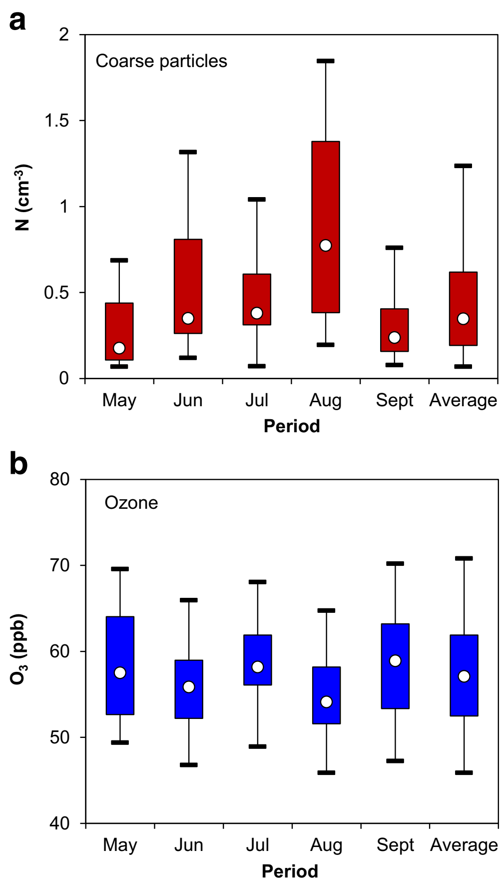


**Fig. 3** Box plots of coarse particles (d > 1 μm) (**a**) and ozone (**b**) at Mt. Aitana during the study period. The whiskers correspond to the 25th and 75th percentiles, and the *round inside de box* represents the median value. Maximum and minimum concentrations are represented by *dashes*

The less solar radiation registered in August in relation to July (see Table 1) may justify the decrease in ozone levels recorded in August. Nevertheless, it does not justify the lower ozone value obtained in August compared with the one recorded in September, since September shows the SR lowest value (see Table 1). For that reason, the low ozone concentration recorded in August could be also attributed to the large number of days that were under the influence of Saharan air masses during this month (see Table 2 in the next section).

In Fig. 4, hourly average patterns of coarse particles and ozone concentrations recorded at sampling point during the study period are shown.

Particle mean concentration was 0.45 ± 0.05 $cm^{-3}$, more than double the concentration recorded in the autumn-winter period of the same year (data not shown) and higher than the values obtained in summer in similar environments such as Mt. Cimone (2165 m a.s.l., 0.25 $cm^{-3}$; Marinoni et al. 2008). This is likely due to the fact that spring and summer 2012 were particularly intense in SDOs along with other processes such as formation of secondary particles and convective resuspension. Also, as aforementioned, the sampling site remains for an elevated percentage of days during the summer period within the PBL meaning it can be influenced by the recirculation of air masses from the coast. Regarding the hourly evolution, particle concentration reached its maximum between 11:00 and 16:00 UTC and began to decrease about 20:00 UTC. This behavior has already been observed in stations with similar altitude (Marinoni et al. 2008).

Ozone mean concentration was 57.7 ± 0.2 ppb. The hourly evolution shows the typical ozone profile that takes place in high altitude locations. That is, it shows a lower oscillation of levels throughout the day and higher average concentrations with respect to stations located in lower altitudes. This ozone behavior in mountain stations can be confirmed in the EMEP/CCC-Report 2/2014 (http://www.nilu.no/projects/ccc/reports.html). The major cause of the absence of a marked diurnal trend in mountain sites is because these sites are not affected by direct emissions. In addition, in these places located close to the Mediterranean coast during the spring-summer period, we must consider that ozone concentrations do not decrease significantly at night since they stay in contact with the stratified air masses rich in ozone that are found in upper layers (Millán et al. 2002; Caballero et al. 2007). However, the ozone evolution presented a maximum hourly oscillation (maximum value—minimum value) of 10 %. The maximum ozone concentration was reached about 19:00 UTC and took place with some delay compared with solar radiation. On summer days, the typical sea breezes bring the pollutants inland while strong sun insolation promotes their transformation into $O_3$ and other photochemical oxidants (Caballero et al. 2007). As such, this delay is probably due to the transport and new photochemical production from precursors emitted along the coast up to the sampling point. This fact has been seen in other studies performed in the Mediterranean basin (Millán et al. 2000). Minimum levels were recorded at 10:00 UTC, and there was no significant decrease in concentration levels during the night (>56 ppb), considering that the monitoring site used to be within PBL and is therefore affected by regional recirculations.

## SDOs: effects on particles and ozone

### *Coarse particles increase*

The SDOs identified according to section 2.3 are shown in Table 2. The sampling site was influenced by SDOs for a total of 75 days (~50 % of the entire study period). These Saharan dust events were distributed in 15 different periods (SDO #). The length of them ranged between 1 and 12 days. Between May and September 2012, about 70 % of the total SDOs registered over the whole year took place.

The presence of mineral dust was registered during the months of June and August for 20 and 19 days, respectively, making them the months most affected by SDOs during the

**Table 2** Saharan dust outbreaks recorded from May 2012 to September 2012

| Abbreviate name | Date | Length (days) | Coarse concentration ($cm^{-3}$) during event |
|---|---|---|---|
| SDO 1 | 10 May to 11 May | 2 | 0.10 |
| SDO 2 | 17 May to 19 May | 3 | 0.81 |
| SDO 3 | 26 May to 4 June | 10 | 0.39 |
| SDO 4 | 7 June to 8 June | 2 | 0.31 |
| SDO 5 | 14 June to 20 June | 7 | 0.75 |
| SDO 6 | 24 June to 2 July | 9 | 1.14 |
| SDO 7 | 7 July to 11 July | 5 | 0.36 |
| SDO 8 | 13 July to 14 July | 2 | 0.74 |
| SDO 9 | 17 July | 1 | 0.35 |
| SDO 10 | 22 July | 1 | 0.41 |
| SDO 11 | 25 July to 5 August | 12 | 1.03 |
| SDO 12 | 8 August to 17 August | 10 | 1.21 |
| SDO 13 | 19 August to 21 August | 3 | 0.43 |
| SDO 14 | 28 August to 29 August | 2 | 0.66 |
| SDO 15 | 18 September to 23 September | 6 | 0.58 |

study period. During these months, the most intense intrusions were also recorded (SDO 6 and SDO 12). It is important to note that in the course of a SDO, particles do not always have high concentrations as will be proven later in the article. In some meteorological scenarios, the transport of dust from Saharan desert is carried out at a considerable altitude. In fact, these transport episodes over Europe can reach altitudes of up 6 km without impact on the lower atmospheric levels (Escudero et al. 2005). Also, particle concentration can fluctuate and levels can alternate between periods of time with high intensity and others with a lower impact.

Mean coarse particle concentration during time periods with SDOs was 0.72 $cm^{-3}$, and the maximum hourly value recorded reached 7.20 $cm^{-3}$. In days without SDOs, the coarse particle concentration was much lower (0.25 $cm^{-3}$-mean concentration). To establish the effect that SDOs have on coarse particles, the hourly variation of particle concentration during SDO periods is represented in Fig. 5 for three different levels: the evolution of the mean hourly value (N-mean), the median hourly value (N-median), and the 75th percentile hourly value (N-P75). The evolution of these three statistical parameters has been obtained from the hourly particle concentrations recorded during SDOs. Additionally, the time evolution of the mean value obtained without SDO (N-NSDO) has been represented too.

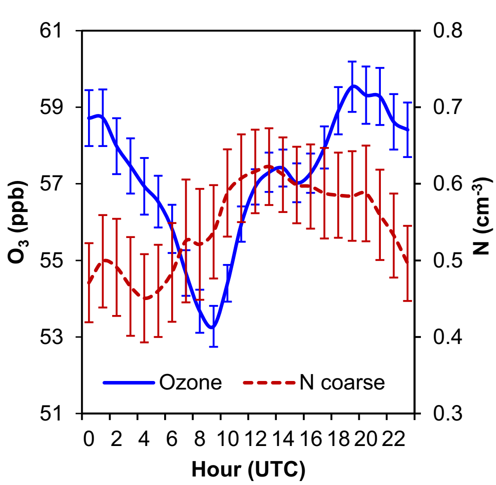


**Fig. 4** Ozone and coarse particles average hourly evolution at sampling point from May to September 2012

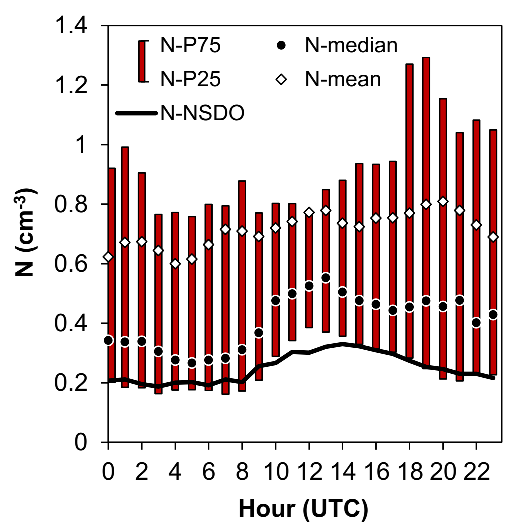


**Fig. 5** Hourly evolution of the mean (*white diamonds*), median (*black rounds*) and range P25–P75 (*box*) values during SDOs and mean hourly variation obtained in periods without Saharan dust

From Fig. 5, it can be seen that the hourly trends of N-median and N-NSDO are quite similar, although N-median shows a noticeable increase after 10:00 UTC. N-P75 and N-mean (in a lower degree) present a progressive increase throughout the day. It seems that the impacts during SDOs periods are more intense during the last hours of the day. In fact, N-P75 presents a clear peak from 18:00 to 23:00 UTC, recording in this time period hourly average concentrations greater than 1 $cm^{-3}$. It is important to point out that this time slot is unique for the SDOs recorded from May to September 2012. In other study periods with other SDOs, the period of day with the highest particle concentrations could be different.

### *Ozone level reductions according to the SDO strength*

In order to determine a particle concentration from which a statistically significant decrease in ozone concentrations is produced, a comparison between hourly ozone average concentrations recorded without SDO ($O_3$-NSDO) and those obtained under SDO has been carried out.

Four different ozone scenarios depending on the particle concentration during a SDO are taken into account: (a) during SDOs independently of the hourly particle concentration ($O_3$-SDO), (b) during SDOs when particle concentration exceeds the median hourly values ($O_3$-N > N-median), (c) during SDOs when particle concentration is above the hourly particle mean values ($O_3$-N > N-mean), and (d) during SDOs when particle concentration is over the P75 hourly particle values ($O_3$-N > N-P75). The hourly values of median, mean, and the P75 are those shown in Fig. 5.

With the ozone concentrations obtained from each of the four intensities, the corresponding ozone percentage reduction ($\downarrow\Delta O_3$ (%)) has been calculated. Moreover, to ascertain when the ozone reduction can be considered significant, a statistical comparison (Mann-Whitney test) has been performed. The ozone concentration obtained without SDO ($O_3$-NSDO) has been used as a reference level. Table 3 shows the results.

**Table 3** Ozone concentrations related to periods without SDOs and periods with SDOs according to four levels of particles intensity: ozone percentage reductions and significance levels

| | Data[a] | $O_3$ ± error (ppb) | $\downarrow\Delta O_3$ (%) | Significance[b] |
|---|---|---|---|---|
| $O_3$-NSDO | 1268 | 58.1 ± 0.2 | | |
| $O_3$-SDO | 1709 | 57.5 ± 0.2 | 1.0 | 0.257 |
| $O_3$-N > N-median | 901 | 55.8 ± 0.2 | 4.0 | 0.000 |
| $O_3$-N > N-mean | 574 | 54.7 ± 0.3 | 5.9 | 0.000 |
| $O_3$-N > N-P75 | 479 | 54.2 ± 0.3 | 6.7 | 0.000 |

[a] Number of hourly records

[b] Levels upper than 0.05, do not reject the null hypothesis ($H_o$), that is, the means are statistically equals between the groups

A statistically significant ozone reduction (4.0 %) is obtained when N > N-median ($p$ value <0.05). Table 3 also reveals that an increase in the particle concentration during SDOs produces a greater decrease in ozone concentrations.

In Fig. 6, the hourly evolution of the main statistical parameters of the ozone concentration obtained during periods without SDOs ($O_3$-NSDO) (Fig. 6a), and those obtained under the influence of SDOs when N > N-mean (Fig. 6b) and N > N-P75 (Fig. 6c) are shown. Hourly evolution of the N-mean, N-P75, and N-NSDO are also shown.

In Fig. 6a, it can be seen that the hourly average concentration and the height of the boxes (P75-P25) show hardly variation (since ozone data did not have a seasonal component). Nevertheless, in Figs. 6b, c, the values of P75-P25 are lower, (meaning the variability of the concentrations is smaller), and present a greater variation in time. In Fig. 6d, the hourly $O_3$ percentage reductions for the two scenarios with higher particle intensity are presented. As can be appreciated, the reduction is maximal between 18:00 and 23:00 UTC. In this time zone, there are percentages of reductions higher than 10 %. Even in the N > N-P75 case, a peak value of ~15 % is reached at 20:00 UTC. In Fig. 5, the reason for this behavior can be found given that in it is during this period of time (18:00–23:00 UTC) when the N-mean and, above all, the N-P75 record their highest values. Thus, during these hours, the impact of SDOs is greater than throughout the rest of the day and therefore the ozone reduction is also higher.

## Ozone reduction characterization and percentages of decrease

In Fig. 7, the hourly variation of ozone and coarse particles recorded during SDO 6 (24 June - 2 July) is shown. Hourly concentrations of N-median are also represented as a reference for particle intensity level for each hour. Likewise, $O_3$-NSDO is also shown. During the fourth and fifth days of the SDO 6 (27 and 28 June), particle levels (N) started to increase and concentrations upper than the N-median (N > N-median) were registered. Meanwhile, ozone concentrations decreased. The ozone decrease is, in this case ~11 ppb. When the Ncoarse > N-median, the ozone decrease is both, steady and statistically significant, lasting until the $O_3$ level reaches its minimum concentration. This depletion takes place in about 36 h. Therefore, ozone concentration presents a decreasing gradient of 0.31 ppb·$h^{-1}$ in this SDO, but it is similar in the most of SDOs. In fact, the decreasing gradients obtained in the remaining SDOs vary from 0.2 to 0.6 ppb $h^{-1}$, with an average value of 0.39 ppb $h^{-1}$.

Moreover, it can be seen that from noon of 29 June and during most of 30 June, particles remained quite high. However, the ozone concentration began to increase progressively, until reaching the $O_3$-NSDO value. Once again, this behavior has been confirmed in most of the SDOs analyzed. It

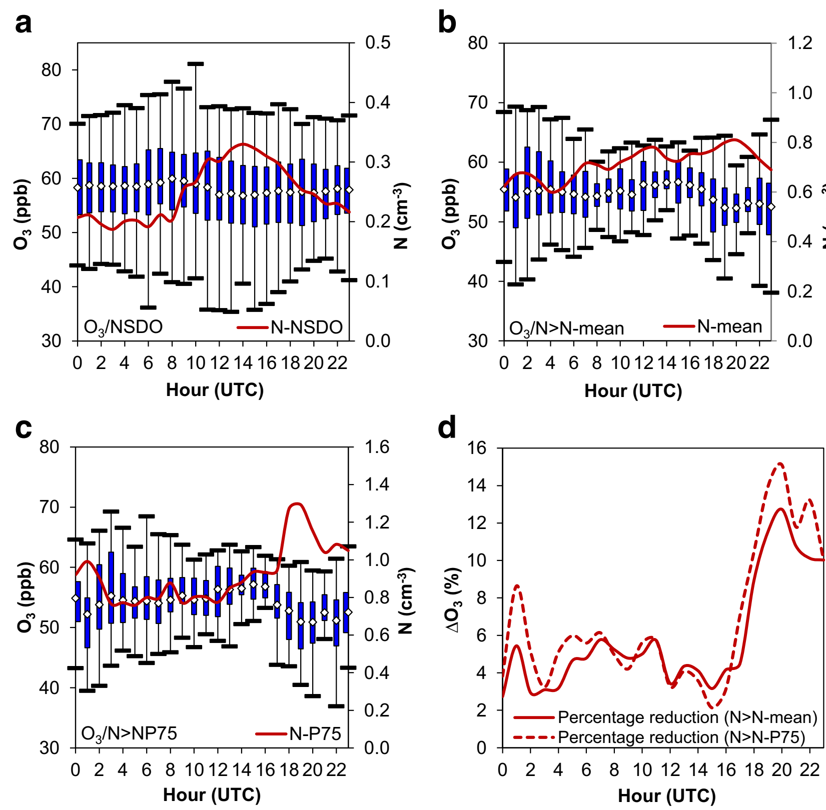


**Fig. 6** Box plot of hourly evolution of ozone at Mt. Aitana during NSDO (**a**), during SDO when N > N-mean (**b**), and when N > N-P75 (**c**). (Maximum and minimum concentrations are represented by *dashes*. The *whiskers* correspond to the 25th and 75th percentiles, and the *diamond inside de box* represents the mean value). **d** Hourly evolution of the ozone difference between $O_3$-NSDO and $O_3$-N > N-mean

is possible that saturation in ozone reduction is produced. This fact can be caused by a complete removal of ozone precursors in the study area. Unfortunately, this statement cannot be verified since the concentrations of the ozone precursors were not measured.

On the whole, during the 9 days that SDO 6 lasted, the ozone mean fell by 4.3 % compared to the ozone mean value recorded without SDOs ($O_3$-NSDO; 58.1 ppb). Approximately, 40 % of the particle data during SDO 6 (98 hourly values) were over the N-mean and 59 % (145 hourly values) over N-median. These levels were recorded mainly in the middle of the Saharan outbreak. The minimum ozone hourly value recorded was 45.7 ppb. This value implies an isolated reduction of 21.3 % in relation to $O_3$-NSDO. In Fig. 7, it is also shown that the highest particle concentration does not coincide with the lowest ozone value.

A summary of the percentages of the ozone reductions for the SDOs identified is shown in Table 4. The percentages have been calculated taking as a reference the $O_3$-NSDO value, 58.1 ppb (see Table 3). Two criteria have been established to quantify these percentages. On the one hand, only ozone values linked to particles whose concentrations are over the N-mean, the N > N-mean, were used. The mean value of ozone when the N > N-mean is also indicated in the table.

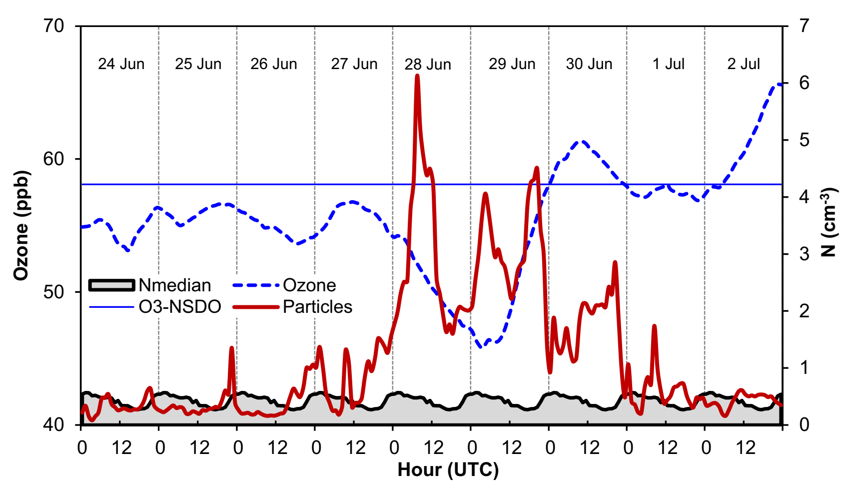


**Fig. 7** Time evolution of hourly concentrations of coarse particles and ozone during SDO 6, from 24 June to 2 July. *Colored area* represents N-median average hourly values

**Table 4** Summary of the percentages of the ozone depletion during SDOs. $O_3$ levels obtained when N > Nmean and minimum $O_3$ hourly values during SDOs

| SDO number | Data[a] | Percentage[b] (N > N-mean) | | | Percentage[c] (minimum $O_3$ hourly value) | | |
|---|---|---|---|---|---|---|---|
| | | N ($cm^3$) | $O_3$ (ppb) | $\Delta O_3$ (%) | N ($cm^3$) | $O_3$ (ppb) | $\Delta O_3$ (%) |
| SDO 2 | 51 (35) | 0.7 | 58.1 | 0.0 | 1.8 | 56.1 | −3.4 |
| SDO 3 | 7 (17) | 1.3 | 57.8 | −0.5 | 0.8 | 55.8 | −4.0 |
| SDO 5 | 37 (63) | 1.3 | 50.0 | −13.9 | 0.7 | 46.0 | −20.8 |
| SDO 6 | 40 (98) | 2.2 | 55.6 | −4.3 | 3.7 | 45.7 | −21.3 |
| SDO 7 | 2 (2) | 1.0 | 59.3 | +2.1 | 0.8 | 58.0 | −0.2 |
| SDO 8 | 28 (14) | 1.1 | 57.8 | −0.5 | 1.0 | 55.4 | −4.7 |
| SDO 9 | 13 (12) | 0.9 | 48.9 | −15.8 | 1.0 | 47.9 | −22.7 |
| SDO 10 | 4 (1) | 1.4 | 53.8 | −7.4 | 1.2 | 52.2 | −10.2 |
| SDO 11 | 50 (146) | 1.6 | 59.5 | +2.4 | 4.8 | 54.7 | −5.9 |
| SDO 12 | 65 (156) | 1.6 | 53.7 | −7.6 | 1.4 | 49.3 | −15.1 |
| SDO 13 | 19 (11) | 1.4 | 52.8 | −9.1 | 0.8 | 50.2 | −13.6 |
| SDO 14 | 40 (20) | 0.9 | 51.8 | −10.8 | 0.7 | 49.0 | −15.7 |
| SDO 15 | 33 (35) | 0.7 | 53.7 | −6.2 | 1.1 | 47.4 | −18.4 |

[a] Percentage (and number) of hourly data that are over N-mean for each SDO

[b] Percentage of ozone depletion when N > N-mean

[c] Percentage of ozone depletion when the minimum hourly value of ozone is registered

On the other hand, the minimum ozone hourly value recorded during the SDO is considered. This value is also indicated in Table 4. During SDO 1 and SDO 4, particle concentration did not exceed the N-mean, for that reason these SDOs are not specified in Table 4. In fact, these SDOs registered the lowest concentrations of coarse particles during the events (see Table 1).

Table 4 shows that the depletion percentages can vary between 0.5 % (SDO 3) and 15.8 % (SDO 9). An average value of the ozone percentage reduction of 5.5 % can be established. These values increase significantly if the minimum hourly value of ozone recorded during the SDO is considered. In these cases, the percentages can reach values higher than 20 % during several outbreaks (SDO 5, SDO 6, and SDO 9). As it was discussed above, the minimum hourly value of ozone does not match the maximum hourly value of particle concentration.

During two SDOs (SDO7 and SDO 11), the percentage obtained, under criterion N > N-mean, increases slightly. This could be related to the high level of ozone registered when, during SDO, particles begin to increase (N > N-mean). Although the ozone reduction occurs, this depletion is not enough to obtain a negative value in $\Delta O_3$.

## Conclusions

The main consequence of the interaction between ozone and mineral dust is a decrease in ozone concentration. Nevertheless, the efficiency of the reduction requires that the mineral dust concentration remains above a threshold value. This study demonstrates that a significant reduction in ozone concentrations is obtained when the hourly particle concentration recorded during dust events exceeds the median hourly values (N > N-median). The study also shows that ozone depletion is more effective during the last hours of the day, from 18:00 to 23:00 UTC. This is due to, in this time period, the greatest impacts of coarse particles during the Saharan dust outbreaks identified have been recorded. Moreover, in the interaction aerosol-ozone, two features have been observed. The first is the time synchronization between the particle increase with the ozone decrease. During the interaction, the ozone concentration presents an average decreasing gradient of 0.39 ppb $h^{-1}$. The second one is the saturation of this reduction with time, although the particle levels remain high.

When particle concentration is higher than the mean hourly value (N > N-mean), during SDOs, an average value of the ozone percentage reduction of 5.5 % for the whole study period can be established. If an isolated SDO is considered, this value can rise beyond 15 %. When evaluating the loss when the minimum hourly ozone value is registered, the percentage can exceed 20 %.

The conclusions drawn in this work motivate a new research in this unique environment. It is essential to continue not only collecting $O_3$ data but also measuring concentrations of $O_3$ precursors. That way, it will be possible to investigate what percentage of $O_3$ depletion is due to its direct uptake in coarse particles and what is caused by the inhibition of the $O_3$ production.

**Acknowledgments** This work was supported by the Spanish Ministry of Science and Innovation under the CGL2009-08036 (PASSE) and CGL2012-39623-C02-2 (PRISMA) projects. We would like to thank the military base (EVA no. 5) for allowing access to its facilities.

## References

Adame JA, Córdoba-Jabonero C, Sorribas M, Toledo D, Gil-Ojeda M (2015) Atmospheric boundary layer and ozone-aerosol interactions under Saharan intrusions observed during AMISOC summer campaign. Atmos Environ 104:205–216

Andrey J, Cuevas E, Parrondo MC, Alonso-Pérez S, Redondas A, Gil-Ojeda M (2014) Quantification of ozone reductions within the Saharan air layer through a 13-years climatologic analysis of ozone profiles. Atmos Environ 84:28–34

Bauer SE, Balkanski Y, Schulz M, Hauglustaine DA (2004) Global modeling of heterogeneous chemistry on mineral aerosol surfaces: influence on tropospheric ozone chemistry and comparison to observations. J Geophys Res 109:D02304. doi:10.1029/2003JD003868

Bencardino M, Sprovieri F, Cofone F, Pirrone N (2011) Variability of atmospheric aerosol and ozone concentrations at marine, urban and high-altitude monitoring stations in southern Italy during 2007 summer Saharan dust outbreaks and wildfire episodes. J Air Waste Manage Assoc 61(9):952–967

Bonasoni P, Cristofanelli P, Calzolari F, Bonafé U, Evangelisti F, Stohl A, Zauli Sajani S, van Dingenen R, Colombo T, Balkanski Y (2004) Aerosol-ozone correlations during dust transport episodes. Atmos Chem Phys 4:1201–1215

Brattich E, Ricccio A, Tossiti L, Cristofanelli P, Bonasoni P (2015) An outstanding Saharan dust event at Mt. Cimone (2165 m a.s.l,, Italy) in March 2004. Atmos Environ 113:223–235

Caballero S, Galindo N, Pastor C, Varea M, Crespo J (2007) Estimated tropospheric ozone levels on the southeast Spanish Mediterranean coast. Atmos Environ 41:2881–2886

Castell-Balaguer N, Téllez L, Mantilla E (2012) Daily, seasonal and monthly variations in ozone levels recorded at the Turia river basin in Valencia (eastern Spain). Environ Sci Pollut Res 19:3461–3348

Contini D, Cesari D, Genga A, Siciliano M, Ielpo P, Guascito MR, Conte M (2014) Source apportionment of size-segregated atmospheric particles based on the major water-soluble components in Lecce (Italy). Sci Total Environ 472:248–261

de Reus M, Dentener F, Thomas A, Borrmann S, Ström J, Lelieveld J (2000) Airbone observations of dust aerosol over the North Atlantic Ocean during ACE 2: indications for heterogeneous ozone destruction. J Geophys Res 105:15263–15275

Dentener FJ, Carmichael GR, Zhang Y, Lelieveld J, Crutzen PJ (1996) Role of mineral aerosol as a reactive surface in the global troposphere. J Geophys Res 101:22869–22889

Dinoi A, Donateo A, Belosi F, Conte M, Contini D (2016) Comparison of atmospheric particle concentration measurements using different optical detectors: potentiality and limits for air quality applications. Measurement. In press. doi:10.1016/j.measurement.2016.02.019

Donateo A, Contini D, Belosi F (2006) Real time measurements of PM2.5 concentrations and vertical turbulent fluxes using an optical detector. Atmos Environ 40:1346–1360

Draxler R.R, Rolph G.D (2015) HYSPLIT (HYbrid Single-Particle Lagrangian Integrated Trajectory) Model access via NOAA ARL READY Website (http://ready.arl.noaa.gov/HYSPLIT.php)

Escudero M, Castillo S, Querol X, Avila A, Alarcon A, Viana MM, Alastuey A, Cuevas E, Rodriguez S (2005) Wet and dry African dust episodes over eastern Spain. J Geophys Res 110:D18S08. doi:10.1029/2004JD004731

Escudero M, Querol X, Avila A, Cuevas E (2007) Origin of exceedances of the European daily PM limit value in regional background áreas of Spain. Atmos Environ 41:730–744

Escudero M, Lozano A, Hierro J, del Valle J, Mantilla E (2014) Urban influence on increasing ozone concentrations in a characteristic Mediterranean agglomeration. Atmos Environ 99:322–332

Escudero M, Lozano A, Hierro J, Tapia O, del Valle J, Alastuey A, Moreno T, Anzano J, Querol X (2016) Assessment of the variability of atmospheric pollution in National Parks of mainland Spain. Atmos Environ 132:332–344

Galindo N, Yubero E, Nicolás JF, Crespo J, Soler R (2016) Chemical characterization of PM1 at a regional background site in the western Mediterranean. Aerosol Air Qual Res 16:530–541

Hanisch F, Crowley JN (2003) Ozone decomposition on Saharan dust: an experimental investigation. Atmos Chem Phys 3:119–130

Harrison SP, Kohfeld KE, Roelandt C, Claquin T (2001) The role of dust in climate changes today, at the last glacial maximum and in the future. Earth Sci Rev 54:43–80

IPCC (Intergovernmental Panel on Climate Change) (2013) The Physical Science Basis. Contribution of Working Group I to the Fifth Assessment Report of the Intergovernmental Panel on Climate Change. Cambridge University press

Lelieveld J, Berresheim H, Borrmann S, Crutzen PJ, Dentener FJ, Fischer H, Feichter J, Flatau PJ, Heland J, Holzinger R, Korrmann R, Lawrence MG, Levin Z, Markowicz KM, Mihalopoulos N, Minikin A, Ramanathan V, de Reus M, Roelofs GJ, Scheeren HA, Sciare J, Schlager H, Schultz M, Siegmund P, Steil B, Stephanou EG, Stier P, Traub M, Warneke C, Williams J, Ziereis H (2002) Global air pollution crossroads over the Mediterranean. Science 298:794

Marinoni A, Cristofanelli P, Calzolari F, Roccato F, Bonafè U, Bonasoni P (2008) Continuous measurements of aerosol physical parameters at the Mt. Cimone GAW Station (2165 m asl, Italy). Sci Total Environ 391:241–251

Millán MM, Mantilla E, Salvador R, Carratalá A, Sanz MJ, Alonso L, Gangoiti G, Navazo M (2000) Ozone cycles in the western Mediterranean Basin: interpretation of monitoring data in complex coastal terrain. J Appl Met 39:487–508

Millán MM, Sanz MJ, Salvador R, Mantilla E (2002) Atmospheric dynamics and ozone cycles related to nitrogen deposition in the western Mediterranean. Environ Pollut 118(2):167–186

Monks PS (2000) A review of the observations and origins of the spring ozone maximum. Atmos Environ 34:3545–3561

Nicolás JF, Crespo J, Yubero E, Soler R, Carratalá A, Mantilla E (2014) Impacts on particles and ozone by transport processes recorded at urban and high-altitude monitoring stations. Sci Total Environ 466–467:439–446

Paoletti E (2006) Impact of ozone on Mediterranean forests: a review. Environ Pollut 144(2):463–474

Pio C, Cardoso J, Cerqueira M, Calvo A, Nunes T, Alves C, Custodio, D, Almeida S, Almeida-Silva M (2014) Seasonal variability of aerosol concentration and size distribution in Cape Verde using a continuous aerosol optical spectrometer. Front Environ Sci 2–15. doi: 10.3389/fenvs.2014.00015

Prospero JM, Schmitt R, Cuevas E, Savoie D.L, Graustein WC, Turekian KK, Volz-Thomas A, Diaz A, Oltmans SJ, Levy II H (1995) Temporal variability of summer-time ozone and aerosol in the free troposphere over the eastern North Atlantic. Geophys Res Lett 22, 21:2925–2928

Pey J, Querol X, Alastuey A, Forastiere F, Stafoggia M (2013) African dust outbreaks over the Mediterranean Basin during 2001–2011: $PM_{10}$ concentrations, phenomenology and trends, and its relation with synoptic and mesoscale meteorology Atmos. Chem Phys 13: 1395–1410

Querol X, Alastuey A, Pey J, Escudero M, Castillo S, Gonzalez A, Pallares M, Jiménez S, Cristobal A, Ferreira F, Marques F, Monjarino J, Cuevas E, Alonso S, Artiñano B, Salvador P, de la Rosa J (2006) Spain and Portugal Methodology for the identification of natural African dust episodes in $PM_{10}$ and $PM_{2.5}$, and justification with regards to the exceedances of the $PM_{10}$ daily limit value. Ministerio de Medio Ambiente, Medio Rural y Marino (Spain) and Ministério do Ambiente, Ordenamento do Territorio e Desenvolvimento Regional (Portugal) 32 pp

Querol X, Pey J, Pandolfi M, Alastuey A, Cusack M, Pérez N, Moreno T, Viana MM, Mihalopoulos N, Kallos G, Kleanthous S (2009) African dust contributions to mean ambient $PM_{10}$ mass-levels across the Mediterranean Basin. Atmos Environ 43:4266–4277

Ribas A, Peñuelas J (2004) Temporal patterns of surface ozone levels in different habitats of the north western Mediterranean basin. Atmos Environ 38:985–992

Umann B, Arnold F, Schaal C, Hanke M, Uecker J, Aufmhoff H, Balkanski Y, Van Dinengen R (2005) Interaction of mineral dust with gas phase nitric acid and sulfur dioxide during the MINATROC II field campaign: first estimate to the uptake coefficient gamma ($HNO_3$) from atmospheric data. J Geophys Res 110(D22306). doi:10.1029/2005JD005906

Zhang Y, Carmichael GR (1999) The role of mineral aerosol in tropospheric chemistry in East Asia-a model study. J Appl Met 38:353–366

Zhang Y, Sunwoo Y, Kotamarthi V, Carmichael GR (1994) Photochemical oxidant processes in the presence of dust. An evaluation of the impact of dust on particle nitrate and ozone formation. J Appl Met 33:813–824